Photoneutron cross sections for ^{96}Zr: A systematic experimental study of photoneutron and radiative neutron capture cross sections for zirconium isotopes

H. Utsunomiya,[1] S. Goriely,[2] H. Akimune,[1] H. Harada,[3] F. Kitatani,[3] S. Goko,[3] H. Toyokawa,[4] K. Yamada,[4] T. Kondo,[1] O. Itoh,[1] M. Kamata,[1] T. Yamagata,[1] Y.-W. Lui,[5] S. Hilaire,[6] and A. J. Koning[7]

[1]*Department of Physics, Konan University, Okamoto 8-9-1, Higashinada, Kobe 658-8501, Japan*

[2]*Institut d'Astronomie et d'Astrophysique, Université Libre de Bruxelles, Campus de la Plaine, CP-226, B-1050 Brussels, Belgium*

[3]*Japan Atomic Energy Agency, Tokai-mura, Naka, Ibaraki 319-1195, Japan*

[4]*National Institute of Advanced Industrial Science and Technology, Tsukuba 305-8568, Japan*

[5]*Cyclotron Institute, Texas A&M University, College Station, Texas 77843, USA*

[6]*Département de Physique Théorique et Appliquée, Service de Physique Nucléaire, B.P. 12 F-91680 Bruyères-le-Châtel, France*

[7]*Nuclear Research and Consultancy Group, P.O. Box 25, NL-1755 ZG Petten, The Netherlands*

(Received 21 December 2009; published 15 March 2010)

Photoneutron cross sections were measured for ^{96}Zr near neutron threshold with quasimonochromatic laser-Compton-scattering γ-ray beams. A systematic analysis of photoneutron and radiative neutron capture data for zirconium isotopes within the statistical model calculation leads to a unified picture of low-energy γ-ray strengths for zirconium isotopes that is described by the HFB + QRPA model of $E1$ strength supplemented with an extra γ strength attributed to a giant $M1$ resonance. Results of the systematic analysis including radiative neutron capture cross sections for radioactive ^{95}Zr and ^{93}Zr nuclei are presented.

DOI: 10.1103/PhysRevC.81.035801 PACS number(s): 25.20.−x, 21.10.Pc, 24.30.Gd, 27.60.+j

I. INTRODUCTION

The radiative neutron capture cross section for short-lived radioactive nuclei is difficult to measure due to the fact that the measurement requires both highly radioactive samples and an intense neutron source. ^{95}Zr with the half-life of $T_{1/2} =$ 64 days is one of such nuclei for which experimental data are currently unavailable. The scientific interest in radiative neutron capture cross sections for ^{95}Zr is twofold. First, it is an s-process branching point nucleus at which the s-process nucleosynthesis path splits into neutron capture to ^{96}Zr and β-decay to ^{95}Mo via ^{95}Nb [1]. Second, the recent analyses of type X SiC grains showed anomalies in the isotopic patterns of Mo with excesses in ^{95}Mo and ^{97}Mo [2,3] and Zr with an excess in ^{96}Zr [3], respectively. The isotopic patterns differ from those expected from the pure r and s process, suggesting that the X SiC grains are so-called supernova condensates that were exposed to a moderate neutron burst [4].

Photodisintegration is an excellent probe of the γ-ray strength function, $f(E_\gamma)$, which is an essential ingredient for describing γ decays of a neutron captured state assuming the equality between $f(E_\gamma)\downarrow$ and $f(E_\gamma)\uparrow$ known as the Brink hypothesis [5]. Therefore, photodisintegration can be used to improve the prediction of the radiative neutron capture cross section by experimentally constraining the γ-ray strength function $f(E_\gamma)$ entering the statistical model calculation.

We have so far measured photoneutron cross sections for ^{91}Zr, ^{92}Zr, and ^{94}Zr isotopes [6]. We recently carried out a new measurement for ^{96}Zr near the neutron threshold (S_n) at 7.85 MeV. We perform a coherent analysis of all the available photoneutron cross sections $\sigma_{\gamma n}$ and radiative neutron capture cross sections $\sigma_{n\gamma}$ for Zr isotopes with emphasis on the model prediction of $\sigma_{n\gamma}$ for two radioactive isotopes, ^{95}Zr and ^{93}Zr. The latter cross section is important from the viewpoint of nuclear transmutation of the long-lived fission product ^{93}Zr with $T_{1/2} = 1.5 \times 10^6$ y. Experimental details are given in Sec. II. Section III gives results of the measurement. The model prediction including a systematic analysis of both the neutron capture and photoneutron channels are given and discussed in Sec. IV. A summary is given in Sec. V.

II. EXPERIMENT

Quasimonochromatic γ-ray beams produced in the laser Compton scattering (LCS) at the National Institute of Advanced Industrial Science and Technology (Japan) were used to irradiate a metallic powder of 1342 mg/cm^2 of ^{96}Zr (86.4 ± 0.6% in atomic percent). Isotopic impurities in the ^{96}Zr sample were ^{90}Zr (5.0%), ^{91}Zr (1.88%), ^{92}Zr (2.69%), and ^{94}Zr (4.03%). Photoneutrons were measured at 12 maximum energies of the LCS γ-ray beam from 8.1 to 14.0 MeV. The beam energy was tuned by changing the electron beam energy from 480.3 to 633.2 MeV.

The experimental procedure was the same as described in Refs. [7,8] except for two aspects: the determination of the energy distribution of the LCS γ-ray beam and the experimental subtraction of neutron events attributed to isotopic impurities. The LCS γ-ray beam was measured with the high-resolution high-energy photon spectrometer (HHS) [9] at a reduced laser power before and after the neutron measurements. The HHS consists of two 334 cm^3 high-purity Ge detectors shielded with an array of 23 pieces of BGO crystals with a total volume 11.8×10^3 cm^3 [9,10]. The response function of the HHS was measured with the standard γ-ray sources and 10.763 MeV γ rays produced in the ^{27}Al + p reaction at 1012 keV and well simulated by taking into account the surface channel effect [11,12]. Energy spectra measured with the HHS were unfolded with the known response function to determine the energy distributions of the LCS γ-ray beam. Figure 1 shows an example of the unfolded spectrum as well as the pulse-height spectrum of the HHS to the LCS γ-ray beam.

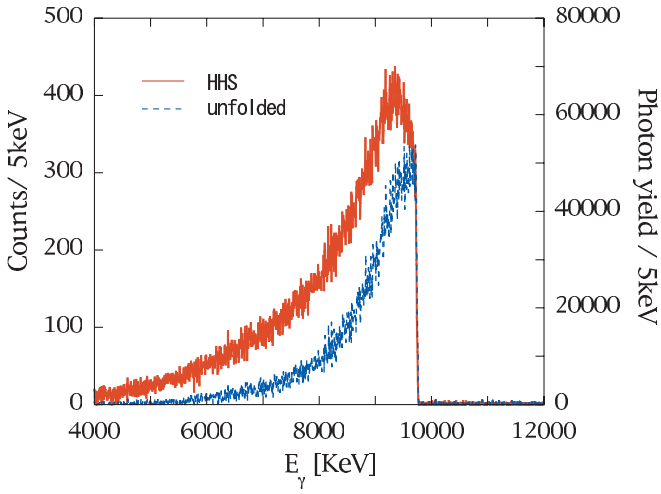

FIG. 1. (Color online) An energy spectrum of the LCS γ-ray beam measured with the high-resolution high-energy photon spectrometer (solid line) and its unfolded spectrum (dotted line).

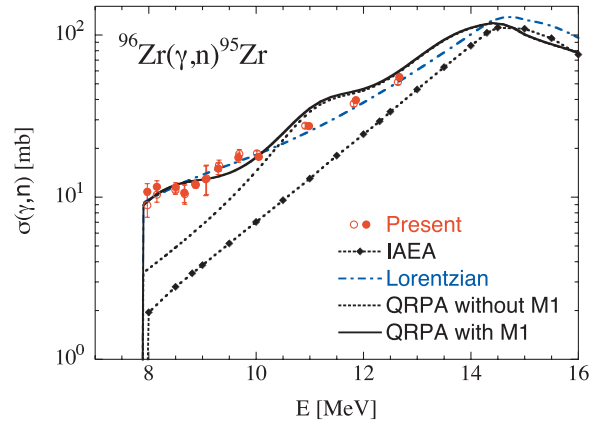

FIG. 2. (Color online) Comparison of experimental and theoretical ^{96}Zr$(\gamma,n)^{95}$Zr cross sections. The solid (dotted) line corresponds to the QRPA calculation with (without) the $M1$ component, as discussed in the text. The dash-dot line is obtained with a pure Lorentzian model. The diamonds corresponds to the cross section recommended by the IAEA handbook [14].

Neutron events originated from the isotopic impurities were experimentally subtracted by using enriched samples of ^{90}Zr (97.7%, 2249 mg/cm^2), ^{91}Zr (90.4%, 1751 mg/cm^2), ^{92}Zr (91.4%, 1601 mg/cm^2), and ^{94}Zr (92.6%, 1835 mg/cm^2) in the chemical form ZrO_2. The separate measurement for impurity nuclei was made whenever the γ-ray energy exceeded the neutron thresholds of impurities nuclei ($S_n = 11.97$ MeV for ^{90}Zr, 7.19 MeV for ^{91}Zr, 8.63 MeV for ^{92}Zr, 8.22 MeV for ^{94}Zr). The contribution from the isotopic impurities was determined by normalizing the relevant numbers of impurity nuclei and incident γ rays to those for the ^{96}Zr runs. The contribution from the isotopic impurities to neutron events amounted to 1.4–11.5%.

Uncertainties of the cross section associated with the time variation of the energy distribution of the LCS γ-ray beam were as large as 10% for long runs near neutron threshold and was negligible otherwise. The systematic uncertainty for the cross section is 4.4–10.8% which represents a quadratic sum of uncertainties of the neutron detection efficiency (3.2%), the number of incident γ rays (3%) and the time variation of the LCS beam energy distribution.

III. ^{96}Zr PHOTONEUTRON CROSS SECTION

Photoneutron cross sections were deduced with the χ^2-fitting method and the Taylor expansion method [7,13]. The two data-reduction methods provide consistent cross sections. The results are shown in Fig. 2 by the open circles for the χ^2 fitting and solid circles for the Taylor expansion methods. The experimental cross section has been compared with theoretical calculations in the same line as in Ref. [6], i.e., on the basis of the TALYS code [15] making use of different $E1$ and $M1$ γ-ray strength prescriptions. In our previous analysis, an extra γ strength was systematically identified for the three ^{91}Zr, ^{92}Zr, and ^{94}Zr isotopes in the photoneutron channel on top of the $E1$ strength estimated by the HFB + QRPA model calculation [16]. This additional strength was associated with an $M1$ resonance at $E_0 \simeq 9$ MeV with a width $\Gamma \simeq 2.5$ MeV and a peak cross section $\sigma_0^{M1} \simeq 7$ mb in Lorentz shape. The energy-integrated $M1$ cross section amounts to ~2% of the giant-dipole-resonance (GDR) cross section of the Thomas-Reiche-Kuhn (TRK) sum rule. This specific description of the γ strength was found to reproduce not only the photoneutron cross section but also the reverse radiative neutron capture cross section which is sensitive to the strength function below the neutron threshold. In contrast, the traditional Lorentzian approximation of the $E1$ strength without any extra low-energy dipole strength was shown to give a very accurate description of the photoneutron cross section on the one hand but to result in an unacceptable overestimate of the reverse (n,γ) cross sections on the other hand.

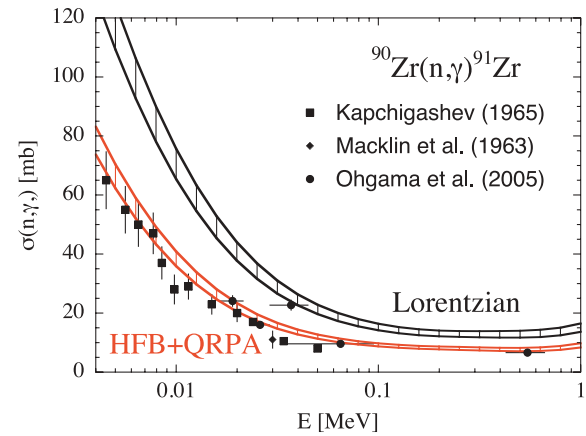

FIG. 3. (Color online) Comparison of experimental and theoretical ^{90}Zr$(n,\gamma)^{91}$Zr cross sections. The theoretical curves were obtained with the $E1$ HFB + QRPA strength [16] supplemented with a strong $M1$ resonance as well as with the standard Lorentzian for both the $E1$ and $M1$ strengths, as recommended in Ref. [17]. The error bars on the theoretical estimate are obtained using different nuclear level-density prescriptions. The experimental data are from Refs. [18–20].

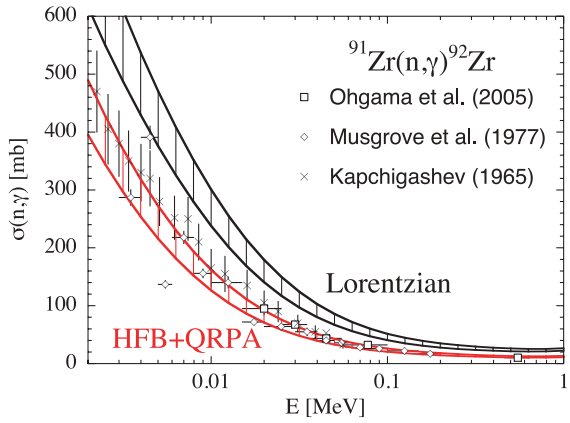

FIG. 4. (Color online) Same as Fig. 3 for ^{91}Zr(n,γ)^{92}Zr. Experimental data are taken from Refs. [18,21,22].

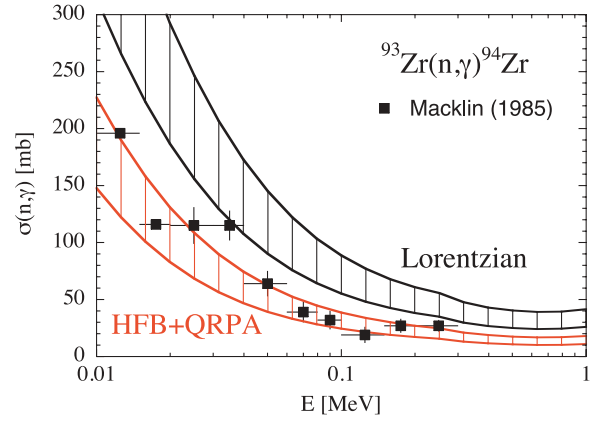

FIG. 6. (Color online) Same as Fig. 3 for ^{93}Zr(n,γ)^{94}Zr. Experimental data are taken from Ref. [23].

As can be seen in Fig. 2, the cross section based on the HFB + QRPA $E1$ strength and a strong $M1$ component also reproduces fairly well the experimental ^{96}Zr(γ,n)^{95}Zr cross section, as does the Lorentzian model [17] with an adjusted width of 4.5 MeV. In contrast the new experimental data are seen not to be compatible with the cross section recommended by the systematic IAEA analysis [14].

IV. SYSTEMATIC ANALYSIS

The analyses made in the present article and in our previous publication [6] provide rather strong constraints on the γ-ray strength in the vicinity of the neutron threshold for all the Zr isotopes. We have shown systematically that either of the standard $E1$ plus $M1$ Lorentzian [17] and the HFB + QRPA [16] $E1$ strength accompanied by a rather strong $M1$ resonance could reproduce rather well the photoneutron data. From such systematic analyses, it is now also possible to provide a detailed examination of the reverse radiative neutron capture cross section and to study the capacity of the above-mentioned models to describe (n,γ) and (γ,n) channels simultaneously. In Ref. [6], only the ^{91}Zr(n,γ)^{92}Zr reaction was treated. We now compare in Figs. 3–8 experimental and calculated cross sections for all the Zr targets for which experimental data is available. The comparison was made over the so-called resolved-resonance and unresolved-resonance regions, where the statistical nature of neutron capture is expected to dominate. Note that the first resonance appears at a few keV in the neutron capture on ^{90,92,94}Zr and at sub-keV energies in the neutron capture on ^{91,93,96}Zr [24]. The keV radiative neutron capture cross section is known to be sensitive not only to the γ-ray strength but also to the nuclear level density (at such energies the cross section remains insensitive to the optical model potential). However, for the ^{91,92,93,94,95,97}Zr isotopes, experimental s-wave resonance spacings at the neutron binding energy as well as excited level spectra exist [17] and can significantly constrain the nuclear level density below the neutron separation energy. Different level-density models, as described in Ref. [25], are used to estimate the sensitivity of the (n,γ) cross section with respect to level densities. The corresponding sensitivity is depicted by the hashed areas in Figs. 3–8.

In the six capture reactions considered here, the HFB + QRPA model (with an enhancement by a strong $M1$ resonance) is found to give systematically a much better agreement with experimental data than does the Lorentzian model which always overestimates the cross section, as already

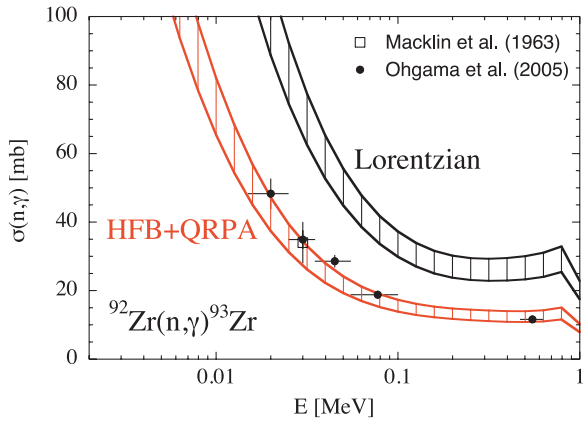

FIG. 5. (Color online) Same as Fig. 3 for ^{92}Zr(n,γ)^{93}Zr. Experimental data are taken from Refs. [19,21].

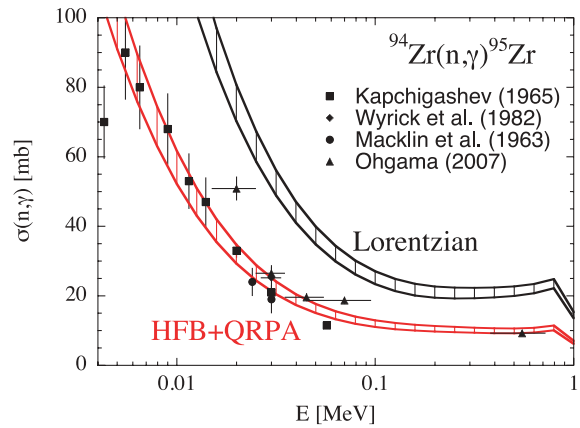

FIG. 7. (Color online) Same as Fig. 3 for ^{94}Zr(n,γ)^{95}Zr. Experimental data are taken from Refs. [18,19,26,27].

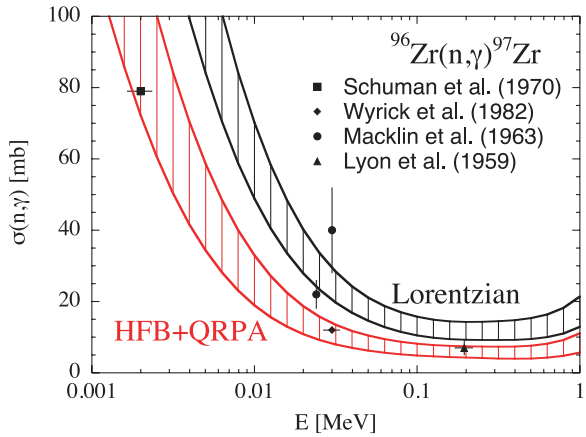

FIG. 8. (Color online) Same as Fig. 3 for ^{96}Zr(n,γ)^{97}Zr. Experimental data are taken from [19,26,28,29].

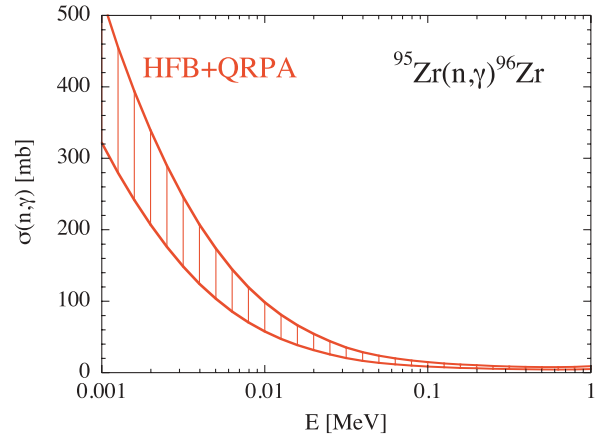

FIG. 9. (Color online) Same as Fig. 3 for ^{95}Zr(n,γ)^{96}Zr. The HFB + QRPA ^{96}Zr γ-ray strength is constrained by the photoneutron data given in Fig. 2.

found for the ^{91}Zr(n,γ)^{92}Zr reaction in Ref. [6] (see also Fig. 4). For the n captures on ^{92}Zr and ^{96}Zr, such a conclusion might be more difficult to draw, since no photoabsorption or photoneutron data exist for ^{93}Zr and ^{97}Zr to constrain the $E1$ strength. Thanks to the existence of data for neighboring nuclei, some confidence can be expected from the systematics, at least for ^{92}Zr. For the n capture on ^{96}Zr, the neutron threshold for ^{97}Zr is low (5.6 MeV), which makes the predictions even more uncertain. In both cases, the same trend for the cross sections is observed, even if large uncertainties still seem to affect the neutron capture data.

On the basis of our new photoneutron data (Fig. 2) and the systematic (n,γ) data analysis, it is possible to use exactly the same input models to estimate the ^{95}Zr(n,γ)^{96}Zr cross section with a relative confidence. We show in Fig. 9 the cross-section predictions. The hashed area reflects the expected uncertainty stemming from the level densities (see discussion above) and the exact location of the $M1$ resonance around 8 to 9 MeV. This latter range is found to be compatible with the photoneutron data in Fig. 2. Here also the Lorentzian would give a higher cross section.

V. SUMMARY

Photoneutron cross sections were measured for ^{96}Zr near the neutron threshold with the laser Compton scattering γ-ray beams. Using available photoneutron and radiative neutron capture cross sections as experimental constraints on the γ strength function above and below the neutron threshold, respectively, low-energy γ-ray strengths for zirconium isotopes are systematically investigated. A unified picture of the low-energy γ-ray strength function that consists of the HFB + QRPA model of $E1$ strength and a rather strong extra strength (∼2% of the TRK sum rule for GDR) attributable to giant $M1$ resonance is deduced. It is shown that the statistical model calculation with the unified γ-ray strength function reproduces the existing data of (γ,n) and (n, γ) for zirconium isotopes satisfactorily. In contrast, whereas the standard Lorentzian model of the γ-ray strength function reproduces experimental photoneutron cross sections alone sufficiently well, it unacceptably overestimates radiative neutron capture cross sections. The radiative neutron capture cross section for the short-lived ^{95}Zr with $T_{1/2} = 64$ days is predicted within the same framework of the statistical model calculation.

ACKNOWLEDGMENTS

We thank M. Igashira for providing us with the radiative neutron capture data for ^{94}Zr. We are indebted to T. Kaihori for his technical assistance in the early stage of the experiment. The present study includes the result of "Study on nuclear data by using a high intensity pulsed neutron source for advanced nuclear system" entrusted to Hokkaido University by the Ministry of Education, Culture, Sports, Science and Technology of Japan (MEXT). This work is partly supported by the Japan Private School Promotion Foundation and the Konan-ULB bilateral project. S.G. acknowledges support from FNRS.

[1] F. Käppeler, H. Beer, and K. Wisshak, Rep. Prog. Phys. **52**, 945 (1989).
[2] M. J. Pellin, A. M. Davis, R. S. Lewis, S. Amari, and R. N. Clayton, Lunar Planet. Sci. Conf. **30**, 1969 (1999).
[3] M. J. Pellin, W. F. Calaway, A. M. Davis, R. S. Lewis, S. Amari, and R. N. Clayton, Lunar Planet. Sci. Conf. **31**, 1917 (2000).
[4] B. S. Meyer, D. D. Clayton, and L.-S. The, Astrophys. J. **540**, L49 (2000).
[5] D. M. Brink, Ph.D. thesis, Oxford University, 1955.
[6] H. Utsunomiya *et al.*, Phys. Rev. Lett. **100**, 162502 (2008).
[7] H. Utsunomiya *et al.*, Phys. Rev. C **80**, 055806 (2009).
[8] A. Makinaga *et al.*, Phys. Rev. C **79**, 025801 (2009).
[9] H. Harada and Y. Sigetome, J. Nucl. Sci. Technol., **32**, 1189 (1995).
[10] Y. Shigetome and H. Harada, Nucl. Instrum. Methods A, **469**, 185 (2001).
[11] H. Harada, K. Furutaka, S. Nakamura, K. Osaka, H. Akimune, H. Utsunomiya, T. Ohsaki, and M. Igashira, Nucl. Instrum. Methods A, **554**, 306 (2005).

[12] H. Utsunomiya, H. Akimune, K. Osaka, T. Kaihori, K. Furutaka, and H. Harada, Nucl. Instrum. Methods A **548**, 455 (2005).
[13] H. Utsunomiya *et al.*, Phys. Rev. C **74**, 025806 (2006).
[14] *Handbook on Photonuclear Data for Applications-Cross Sections and Spectra*, IAEA-TECDOC-1178 (2000).
[15] A. J. Koning, S. Hilaire, and M. C. Duijvestijn, Proc. Int. Conf. on Nuclear Data for Science and Technology, edited by C. Haight *et al.* (AIP, Melville, NY, 2005), Vol. 769, p. 1154.
[16] S. Goriely, E. Khan, and M. Samyn, Nucl. Phys. **A739**, 331 (2004).
[17] T. Belgya *et al.*, *Handbook for Calculations of Nuclear Reaction Data, RIPL-2*, IAEA-Tecdoc-1506 (2006).
[18] S. P. Kapchigashev, Atomnaya Energiya **19**, 294 (1965).
[19] R. L. Macklin, T. Inada, and J. H. Gibbons, Bull. Am. Phys. Soc. **8**, 81 (1963).
[20] K. Ohgama, M. Igashira, and T. Ohsaki, Symp. on Capture Gamma Ray Spectroscopy (AIP, Melville, NY, 2005), Vol. 819, p. 373.
[21] K. Ohgama, M. Igashira, and T. Ohsaki, J. Nucl. Sci. Technol., **42**, 333 (2005).
[22] A. R. Del. Musgrove, J. W. Boldemann, B. J. Allen, J. A. Harvey, and R. L. Macklin, Aust. J. Phys. **30**, 391 (1977).
[23] R. L. Macklin, Astrophys. Space Sci. **115**, 71 (1985).
[24] S. F. Mughabghab, *Atlas of Neutron Resonances—Resonance Parameters and Thermal Cross Sections* $Z = 1$–100, 5th ed. (Elsevier Science, Amsterdam, 2006).
[25] A. J. Koning, S. Hilaire, and S. Goriely, Nucl. Phys. **A810**, 13 (2008).
[26] J. M. Wyrick and W. P. Poenitz, Argonne National Laboratory report series, No. 83, 4, 1982.
[27] K. Ohgama, Ph.D. thesis, Tokyo Institute of Technology, 2007.
[28] R. P. Schuman and R. L. Tromp, Idaho Nuclear Corp. Reports No. 1317, 1970.
[29] W. S. Lyon and R. L. Macklin, Phys. Rev. **114**, 1619 (1959).